**Astronomy & Astrophysics**

# The Solar ALMA Science Archive (SALSA)

## First release, SALAT, and FITS header standard[*]

Vasco M. J. Henriques[1,2], Shahin Jafarzadeh[1,2], Juan Camilo Guevara Gómez[1,2], Henrik Eklund[1,2],
Sven Wedemeyer[1,2], Mikołaj Szydlarski[1,2], Stein Vidar H. Haugan[1,2], and Atul Mohan[1,2]

[1] Rosseland Centre for Solar Physics, University of Oslo, PO Box 1029 Blindern, 0315 Oslo, Norway
e-mail: vh@astro.uio.no
[2] Institute of Theoretical Astrophysics, University of Oslo, PO Box 1029, Blindern 0315, Oslo, Norway

**ABSTRACT**

In December 2016, the Atacama Large Millimeter/submillimeter Array (ALMA) carried out the first regular observations of the Sun. These early observations and the reduction of the respective data posed a challenge due to the novelty and complexity of observing the Sun with ALMA. The difficulties with producing science-ready, time-resolved imaging products in a format familiar to and usable by solar physicists based on the measurement sets delivered by ALMA had limited the availability of such data to this point. With the development of the Solar ALMA Pipeline, it has now become possible to routinely reduce such data sets. As a result, a growing number of science-ready solar ALMA data sets are now offered in the form of the Solar ALMA Science Archive (SALSA). So far, SALSA contains primarily time series of single-pointing interferometric images at cadences of one or two seconds, accompanied by the respective single-dish full-disc solar images. The data arrays are provided in FITS format. We also present the first version of a standardised header format that accommodates future expansions and fits within the scope of other standards including the ALMA Science Archive itself and SOLARNET. The headers include information designed to aid the reproduction of the imaging products from the raw data. Links to co-observations, if available, with a focus on those of the Interface Region Imaging Spectrograph, are also provided. SALSA is accompanied by the Solar ALMA Library of Auxiliary Tools (SALAT), which contains Interactive Data Language and Python routines for convenient loading and a quick-look analysis of SALSA data.

**Key words.** Sun: chromosphere – Sun: general – radio continuum: general

## 1. Introduction

The millimetre wavelength range offers a unique window into the chromosphere of the Sun. In contrast to other chromospheric diagnostics, such as spectral lines, which are typically affected by deviations from local thermodynamic equilibrium (LTE) conditions, the assumption of LTE is believed to be valid for the radiation continuum at millimetre wavelengths as it is formed by thermal bremsstrahlung (free-free emission) (see, e.g. Valle Silva et al. 2021; Wedemeyer et al. 2016; White et al. 2006; Dulk 1985, and references therein). The formation process of the radiation allows us to use the Rayleigh-Jeans approximation, providing a linear relation between the measured flux density and the brightness temperature, which is under ideal conditions closely connected to the local plasma temperature in the continuum-forming atmospheric layer. A particular complication with observing the chromosphere is that it evolves on dynamical timescales of seconds, and it exhibits ubiquitous fine structure on sub-arcsecond spatial scales. Resolving both simultaneously is technically challenging, especially in view of the relatively long wavelengths and the resulting need of correspondingly very large telescope apertures. The technical requirements, which are essential for exploiting the full potential of the millimetre window for the solar chromosphere, are currently only met by the Atacama Large Millimeter/sub-

millimeter Array (ALMA; Wootten & Thompson 2009). Regular solar observations have been performed by ALMA since 2016. For this purpose, the 12-m array with up to 50 antennas, each with a diameter of 12 m, is combined with the Atacama Compact Array (ACA) with up to 12 7-m antennas. The combined interferometric array is sensitive to brightness temperature variations over spatial scales and orientations according to the array configuration relative to the position of the Sun on the sky. Absolute brightness temperatures are derived by combining the images reconstructed from the interferometric data with additional single-dish scans of the solar disc with up to four total power (TP) antennas. Please refer to Shimojo et al. (2017a) for details on the interferometric part and to White et al. (2017) for more information on the single-dish TP component (see also Bastian 2002; Loukitcheva et al. 2008; Karlický et al. 2011; Bastian et al. 2018, and references therein).

Despite the technical challenges, an increasing number of studies based on ALMA observations of the Sun is being published (see, e.g. Bastian et al. 2017; Shimojo et al. 2017b; Yokoyama et al. 2018; Brajša et al. 2018, 2021; Jafarzadeh et al. 2019, 2021; Rodger et al. 2019; Selhorst et al. 2019; Wedemeyer et al. 2020; da Silva Santos et al. 2020a; Eklund et al. 2020, 2021; Nindos et al. 2020, 2021; Patsourakos et al. 2020; Chintzoglou et al. 2021a; Guevara Gómez et al. 2021, and more). While scientific production using ALMA solar data is clearly picking up, interferometric imaging into stabilised, time-consistent data series in absolute temperature units has remained

---

[*] Movies associated to Figs. 3 and 4 are available at https://www.aanda.org

difficult. Due to the significant differences between solar observations and standard ALMA observations of other astronomical targets, ALMA so far delivers calibrated measurement sets to the observers, or, more precisely, the data together with a prepared calibration script that is to be executed by the recipient. The further processing, which includes the construction of time series of the images, requires significant experience, time, and resources, which has hampered access for solar physicists who are as yet unfamiliar with millimetre data. This difficult situation initiated the development of the Solar ALMA Pipeline (SoAP, Szydlarski et al., in prep.) with the aim of providing easy access to science-ready solar ALMA data to the scientific community. Routine data processing with SoAP has so far resulted in multiple science-ready imaging time series. The original data sets were retrieved from ESO's ALMA Science Archive (ASA[1], Stoehr et al. 2017) from where they can be freely downloaded after the end of the proprietary period.

For the publicly available sets, the calibration scripts were executed and SoAP was applied. All resulting processed data sets that were of sufficient quality are now made available online in the Solar ALMA Science Archive (SALSA), which is complementary to ASA in the sense that it contains science-ready data (see Fig. 1).

Here we present the first version of SALSA, consisting of 26 such sets, the accompanying Solar ALMA Library of Auxiliary Tools (SALAT), and the first version of a header standard for the included FITS data files. The respective single-dish TP full-disc solar images, used for calibration, and of which all but one are also available via ASA in a ready-to-use format, are included. The observational data sets included in the current version of SALSA are briefly described in Sect. 2. A brief summary of the data processing with SoAP and the resulting data products are provided in Sects. 3 and 4, respectively. SALSA and SALAT, together with guidelines for usage, documentation, and acknowledgements are addressed in Sect. 5, followed by a summary and outlook in Sect. 6.

## 2. Observations

Solar observations are performed using a heterogeneous array through the combination of the 12-m array and the ACA with additional, typically simultaneous single-dish full-disc scans of the Sun with several TP antennas. The data provided in the first version of SALSA presented here was obtained during the period from December 2016 to 2018. The observations were performed in Band 3, covering the frequency range between 92 and 108 GHz, and Band 6 with frequencies between 229 and 249 GHz. These frequency ranges correspond roughly to an average wavelength of 3 mm for Band 3 and 1.3 mm for Band 6. The radiation in these bands is dominated by (thermal) free-free continuum emission.

The data sets in SALSA are labelled as Dnn (in this first release D01 to D28; see Table 1). We refer to these labels when discussing slight differences in the sets below. All released sets are constructed from single-pointing observations, with a 12-m array and ACA, and contain time-sequences of absolute brightness temperature maps (in units of Kelvin) at a cadence of 1 or 2 s. The observations cover, with some minor time gaps, durations ranging from minutes to over an hour. The 26 data sets released here are part of the following 11 successful observational projects: 2016.1.00030.S, 2016.1.00050.S, 2016.1.00202.S, 2016.1.00423.S, 2016.1.00572.S, 2016.1.
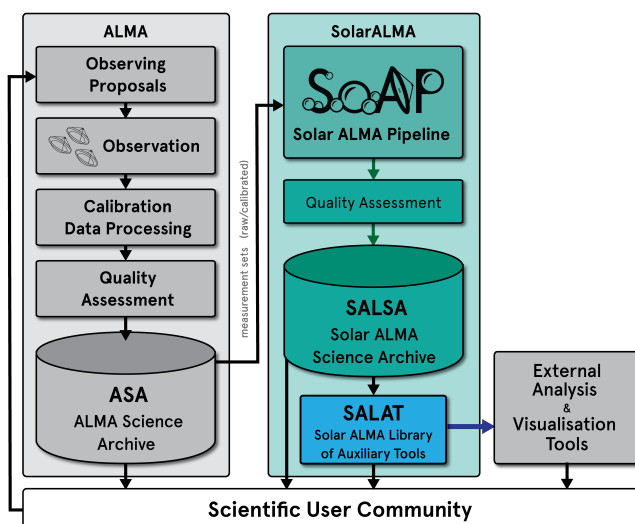
---

**Fig. 1.** While scientists can always download solar measurements sets directly from the ALMA Science Archive, the SolarALMA project created an alternative, which makes access to public, science-ready data easier. The Solar ALMA Science Archive (SALSA) is accompanied by a tool library (SALAT) that also allows the exportation of SALSA data to a format that can be used with other analysis and visualisation tools. Please see the main text for more details.

01129.S, 2016.1.01532.S, 2017.1.00653.S, 2017.1.01672.S, 2018.1.01879.S, and 2018.1.01763.S. The individual observations target quiet-Sun and active regions for a variety of heliocentric angles on the solar disc. An illustrative example of a resulting snapshot in Band 6, close to the disc centre (from D22), is shown in Fig. 2.

All time series display notable evolution for all visible features, including fibrils in some data sets. The included limb data set features a spicule or small protuberance (set labelled as D11). The effective angular resolution of the data sets, as set by the synthesised beam size, which corresponds to the primary lobe of a point-spread function, depends mainly on the wavelength, configuration of the interferometric array, and the position of the target on the sky. Consequently, the effective angular resolution varies significantly between data sets and, to a lesser degree, within the individual time series due to the motion of the Sun across the sky, and potentially from frame to frame for various technical reasons (e.g. flagging of individual antennas).

The ALMA data sets can be aligned (spatially or temporally) with observations from other ground-based or space-borne telescopes (at other wavelengths) to further inspect, for example, the evolution of features of interest at multiple atmospheric heights and for general context. In particular, the Solar Dynamics Observatory (SDO; Pesnell et al. 2012), with continuous observations of the entire solar disc at several wavelength bands (sampling the solar photosphere, low chromosphere, transition region, and corona), can provide complementary information to the ALMA observations (these complement each other since SDO does not sample the chromospheric heights captured by ALMA). Figure 3 shows an example of such alignments between an ALMA image and its co-tempo-spatial images from the Helioseismic and Magnetic Imager (HMI; Schou et al. 2012 and the Atmospheric Imaging Assembly (AIA; Lemen et al. 2012) (onboard SDO) for the first SALSA data set (i.e. D1), taken on 2016 December 22 in Band 3. All SALSA sets are provided with helioprojective coordinates, which should facilitate such alignments. However, the given coordinates and position angles (which allow the rotation

**Table 1.** All datasets present and downloadable in the initial release of SALSA.

| Data | Date | Project ID | Band/λ | Cad. [sec] | Obs. time (UTC) | μ | $T$ mean [K] | Mean resolution [a] bmin/bmaj [arcsec] | Co-Observations | Coordinates [b] | Related publications [c] |
|---|---|---|---|---|---|---|---|---|---|---|---|
| D01 | 2016-12-22 | 2016.1.00423.S | 3/3.0 mm | 2 | 14:19:31-15:07:07 | 0.99 | 7387 ± 519 | 1.37/2.10 | SDO | 0,0 | **1**, **2**, 3, **4**, **17** |
| D02 | 2017-04-22 | 2016.1.00050.S | 3/3.0 mm | 2 | 17:20:13-17:42:37 | 0.92 | 9317 ± 1229 | 1.69/2.21 | IRIS,SDO | −246,267 | 3, **4**, 5, 6, 7, **15** |
| D03 | 2017-04-23 | 2016.1.01129.S | 3/3.0 mm | 2 | 17:19:19-18:52:54 | 0.96 | 7161 ± 1564 | 1.92/2.30 | IRIS,SDO | −54,251 | 3, **4**, 8 |
| D04 | 2017-04-27 | 2016.1.01532.S | 3/3.0 mm | 2 | 14:19:52-15:31:17 | 0.78 | 7974 ± 1145 | 1.74/2.23 | IRIS,SDO | 520,272 | 3, **4** |
| D05 | 2017-04-27 | 2016.1.00202.S | 3/3.0 mm | 2 | 16:00:30-16:43:56 | 0.96 | 7287 ± 1297 | 1.77/1.88 | IRIS,SDO | 172,−207 | 3, **4**, 9, 10 |
| D06 | 2018-04-12 | 2017.1.00653.S | 3/3.0 mm | 1 | 15:52:28-16:24:41 | 0.90 | 7689 ± 661 | 1.77/2.55 | IRIS,SDO | −128,−400 | **4**, 11 |
| D07 | 2017-04-18 | 2016.1.01129.S | 6/1.3 mm | 2 | 14:22:01-15:09:15 | 0.76 | 7167 ± 1158 | 0.75/2.03 | IRIS,SDO | −573,230 | 3, **4**, 8 |
| D08 | 2017-04-22 | 2016.1.00050.S | 6/1.3 mm | 2 | 15:59:17-16:43:26 | 0.92 | 7496 ± 1014 | 0.68/0.85 | IRIS,SDO | −261,266 | 3, **4**, 5, 6, 7 |
| D09 | 2018-04-12 | 2017.1.00653.S | 6/1.3 mm | 1 | 13:58:58-14:32:27 | 0.88 | 5700 ± 333 | 0.80/2.22 | IRIS,SDO | −175,−415 | **4**, 11 |
| D10 | 2018-08-23 | 2017.1.01672.S | 6/1.3 mm | 1 | 16:24:27-17:18:05 | 0.97 | 6104 ± 497 | 1.69/2.21 | IRIS,SDO | 68,−211 | **4** |
| D11 | 2017-03-16 | 2016.1.00572.S | 3/3.0 mm | 1 | 15:22:33-15:32:37 | 0.00 | 7263* ± 148 | 2.55/4.43 | SDO | −679,−679 | 3, 11, 12, 13, 14 |
| D12 | 2017-03-19 | 2016.1.00030.S | 3/3.0 mm | 2 | 18:16:02-19:10:13 | 0.86 | 7364 ± 302 | 2.52/5.06 | IRIS,SDO | −513,−64 | − |
| D15 | 2018-08-23 | 2017.1.01672.S | 6/1.3 mm | 1 | 17:37:00-18:15:57 | 0.87 | 5814 ± 267 | 0.82/1.31 | SDO | 79,−238 | **4** |
| D16 | 2017-03-16 | 2016.1.00572.S | 3/3.0 mm | 2 | 16:58:00-17:06:40 | 0.59 | 7768 ± 186 | 2.70/4.32 | SDO | −517,−585 | 3, 11, 12, 13, 14 |
| D17 | 2017-03-16 | 2016.1.00572.S | 3/3.0 mm | 2 | 18:40:51-18:50:56 | 0.84 | 7510 ± 241 | 2.54/5.17 | IRIS,SDO | −321,−404 | 3, 11, 12, 13, 14 |
| D18 | 2017-03-16 | 2016.1.00572.S | 3/3.0 mm | 2 | 17:59:04-18:09:08 | 0.72 | 7296 ± 251 | 2.52/4.85 | SDO | −468,−484 | 3, 11, 12, 13, 14 |
| D19 | 2017-03-16 | 2016.1.00572.S | 3/3.0 mm | 2 | 19:23:00-19:33:05 | 0.91 | 7416 ± 234 | 2.46/5.77 | SDO | −261,−295 | 3, 11, 12, 13, 14 |
| D20 | 2017-03-16 | 2016.1.00572.S | 3/3.0 mm | 2 | 16:14:48-16:24:53 | 0.13 | 4475 ± 256 | 2.49/4.56 | SDO | −686,−666 | 3, 11, 12, 13, 14 |
| D21 | 2018-12-20 | 2018.1.01763.S | 6/1.3 mm | 1 | 13:19:19-14:07:32 | 0.38 | 6181 ± 208 | 0.60/1.05 | IRIS,SDO | 888,203 | 11 |
| D22 | 2018-12-22 | 2018.1.01879.S | 6/1.3 mm | 1 | 15:09:14-15:14:57 | 1.00 | 6310 ± 185 | 0.73/1.99 | SDO[d] | 1, 0 | − |
| D23 | 2017-04-23 | 2016.1.01129.S | 6/1.3 mm | 2 | 14:23:55-15:11:06 | 0.41 | 6643 ± 396 | 0.71/1.72 | SDO | −860,−129 | 3, **4**, 8 |
| D24 | 2017-03-19 | 2016.1.00030.S | 3/3.0 mm | 2 | 15:32:32-16:26:52 | 0.84 | 7461 ± 421 | 2.65/4.39 | IRIS,SDO | −535,−66 | − |
| D25 | 2017-03-19 | 2016.1.00030.S | 3/3.0 mm | 2 | 16:52:52-17:47:11 | 0.85 | 7387 ± 415 | 2.48/4.31 | IRIS,SDO | −484,−46 | − |
| D26 | 2018-04-12 | 2017.1.00653.S | 3/3.0 mm | 1 | 16:43:52-17:16:06 | 0.90 | 7553 ± 360 | 1.84/2.82 | IRIS,SDO | −131,−400 | **4**, 11, 16 |
| D27 | 2018-04-12 | 2017.1.00653.S | 6/1.3 mm | 1 | 14:51:20-15:25:01 | 0.90 | 5899 ± 157 | 0.89/2.01 | IRIS,SDO | 145,−400 | **4**, 11, 16 |
| D28 | 2017-03-28 | 2016.1.00788.S | 6/1.3 mm | 1 | 15:09:20-16:12:12 | 0.91 | 6157 ± 162 | 1.05/1.89 | IRIS,SDO | −181,347 | 3 |

**Notes.** The date and time of the observations, the associated project ID, receiver band, wavelength, cadence, coordinates (note that coordinates are necessarily approximate and the accuracy depends on the set and visually identifiable features (see text)) and μ angle, mean temperature and respective standard deviation, average resolution given as the time-averaged minor and major axes of the synthesised beam, identified co-observations by IRIS and publications where the set was used as well as publications where the same data were used but processed independently are listed. Publications that used the sets as processed in this database as listed in bold. [a]Time average of the minor and major axes of the clean beam. [b]Necessarily approximate, see text [c]Publications where the SALSA set was used and publications where the data were used but processed independently from this release. [d]DC not targeted by IRIS.

**References.** 1: Wedemeyer et al. (2020); 2: Eklund et al. (2020); 3: Menezes et al. (2021); 4: Jafarzadeh et al. (2021); 5: da Silva Santos et al. (2020b); 6: Chintzoglou et al. (2021a); 7: Chintzoglou et al. (2021b); 8: Molnar et al. (2019); 9: Loukitcheva et al. (2019); 10: Martínez-Sykora et al. (2020); 11: Alissandrakis et al. (2020); 12: Nindos et al. (2018); 13: Patsourakos et al. (2020); 14: Nindos et al. (2020); 15: Guevara Gómez et al. (2021); 16: Nindos et al. (2021); 17: Eklund et al. (2021).
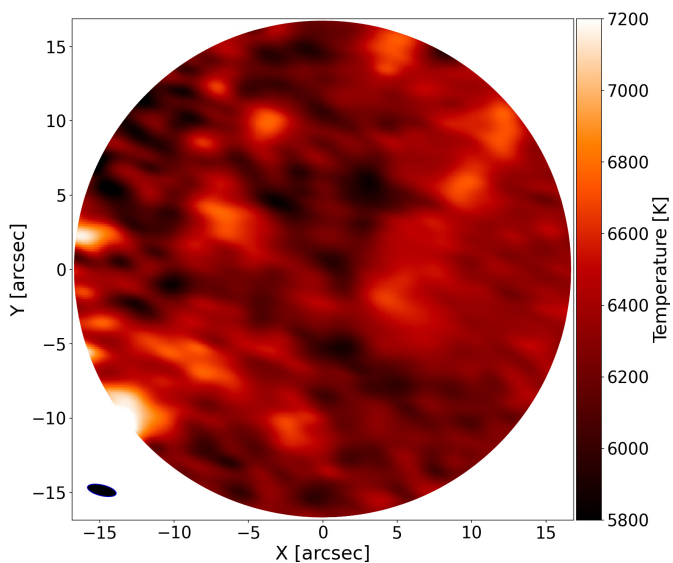


**Fig. 2.** Generic frame from a disc centre set (D22), showing quiet-Sun and network features as observed in Band 6. The elliptic cross-section of the beam shape is plotted in the bottom left of the frame. This plot was made with SALAT (see Sect. 5.2).

of the field of view with respect to the solar north-south direction) may be used only as a first approximation since offsets can be expected (see Sect. 3 for details). It was found that a combination of the SDO/AIA 170 nm and 30.4 nm channels (with different brightness weights) resulted in a similar scene to that sampled by ALMA (in both Bands 3 and 6). For Band 3, adding the SDO/AIA 17.1 nm channel was helpful in some cases. The combined image facilitates cross-correlations between similar solar features with ALMA observations. The field of view illustrated in Fig. 3 samples a magnetically quiescent area, with small network patches (of opposite polarities) as seen in, for example, the HMI magnetogram and the AIA 170 and 160 nm channels. Excess brightness temperature in the ALMA image (at 3.0 mm; Band 3) over the network patches, intensity enhancements in hotter AIA channels over some of these patches, and loops connecting the opposite polarities, are all evident. Larger loops, entering the field of view, are rooted in strong magnetic concentrations outside the target area (see e.g. Wedemeyer et al. 2020 and Jafarzadeh et al. 2021 for detailed analyses of this data set).

Another example of co-observations with other instruments is presented in Fig. 4, where the co-spatial images from the SDO channels and selected images from the Interface Region Imaging Spectrograph (IRIS; De Pontieu et al. 2014) explorer are shown along with the ALMA Band 6 image (from 2017 April
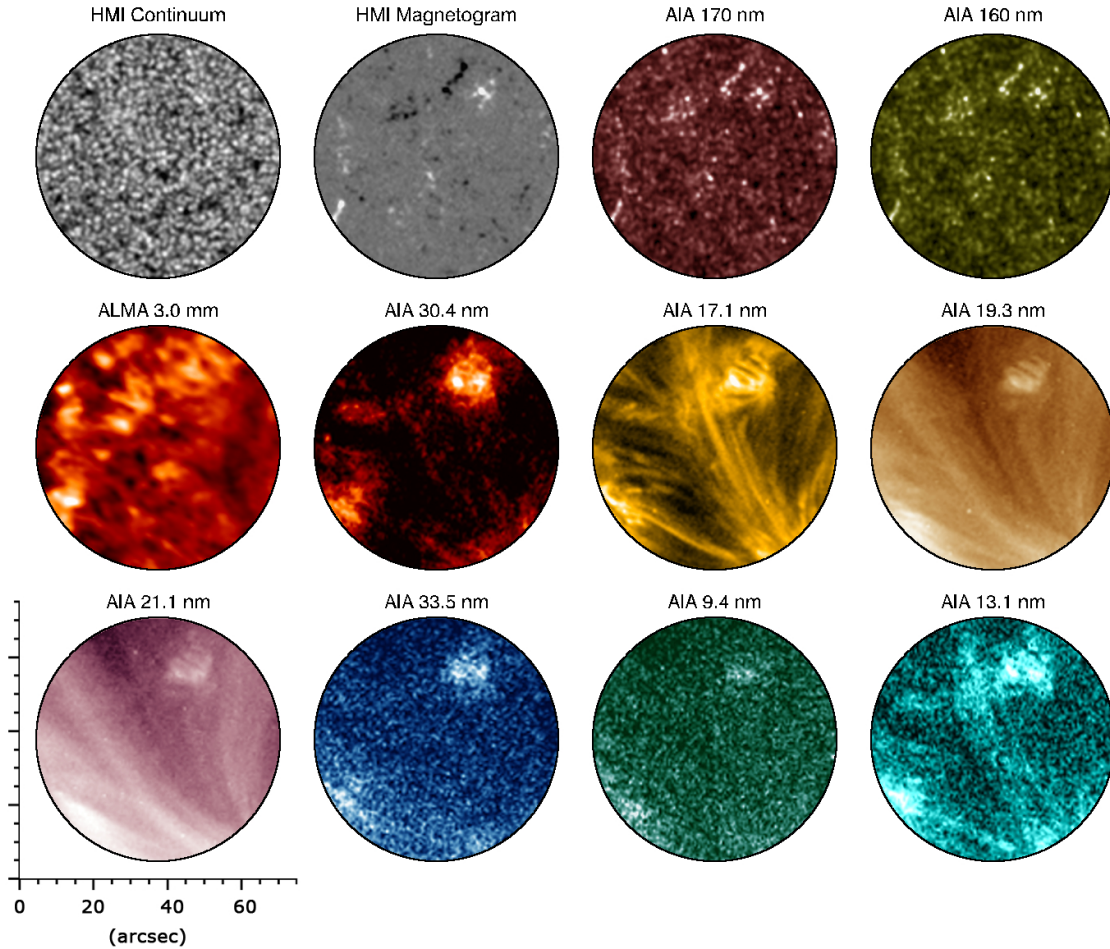
**Fig. 3.** ALMA Band 3 image from 2016 December 22 (project ID 2016.1.00423.S), along with co-aligned SDO images. Time series of images is available online as a movie.

22; D08) at the beginning of the observations. This data set samples a plage or enhanced-network region, with excess brightenings above the magnetic concentrations in the ALMA image, while chromospheric (dark) fibrillar structures (over the internetwork area) are also observed in both ALMA and IRIS Mg II k at 279.61 nm. The latter is a raster image where the slit has scanned a relatively small region compared to that of ALMA. An IRIS slit-jaw image (SJI) at around the Mg II line is also shown in Fig. 4.

The time series of images as shown in Figs. 3 and 4 are available online as a movie. We note that since the ALMA and SDO images were taken with different cadence, the ALMA observations with 2 s cadence was considered as the reference. Hence, the SDO (and IRIS) images are repeated in time to fill in the gaps, in a way that the time difference of the images are the shortest at any given time. These will result in co-alignments of the images both temporally and spatially. It is worth noting that the SDO images in these two examples were resampled to the pixel size of the ALMA images prior to the alignment, but they were not convolved with the synthesised beam of ALMA (i.e. the corresponding PSF). For a one-to-one comparison, such convolutions may be necessary. Necessary routines for extracting a desired ALMA PSF and performing convolutions, along with other useful simple analyses, are provided through the Solar ALMA Library of Auxiliary Tools (SALAT; see Sect. 5.2).

## 3. Data processing

This first release of SALSA is the product of routine application of the Solar ALMA Pipeline (SoAP) to the publicly released measurement sets available on the ALMA Science Archive (ASA, Stoehr et al. 2017). As mentioned above, the primary goal behind SoAP is to simplify processing calibrated ALMA measurement sets into science-ready FITS imaging data. For all data sets, the following steps of SoAP were executed:

1. Imaging including CLEAN wrapper, self-calibration (for all but one data set), and primary-beam correction.
2. Brightness temperature conversion (from Jy/beam to K).
3. Bad frame discarding in time series.
4. Frame-to-frame spatial alignment for ALMA time sequences.
5. Combination of interferometric and total-power data.

The imaging part of SoAP uses the CLEAN algorithm (Högbom 1974) for the deconvolution of images in the form devised by Rau & Cornwell (2011) and as implemented in CASA (Common Astronomy Software Applications; McMullin et al. 2007). The conversion from flux density to brightness temperature was done using the Rayleigh-Jeans approximation of the Planck function and the time-dependent solid angle (i.e. the area covered on the sky) of ALMA's synthesised (elliptical cross-section) beam, following the standard procedure[2].

---

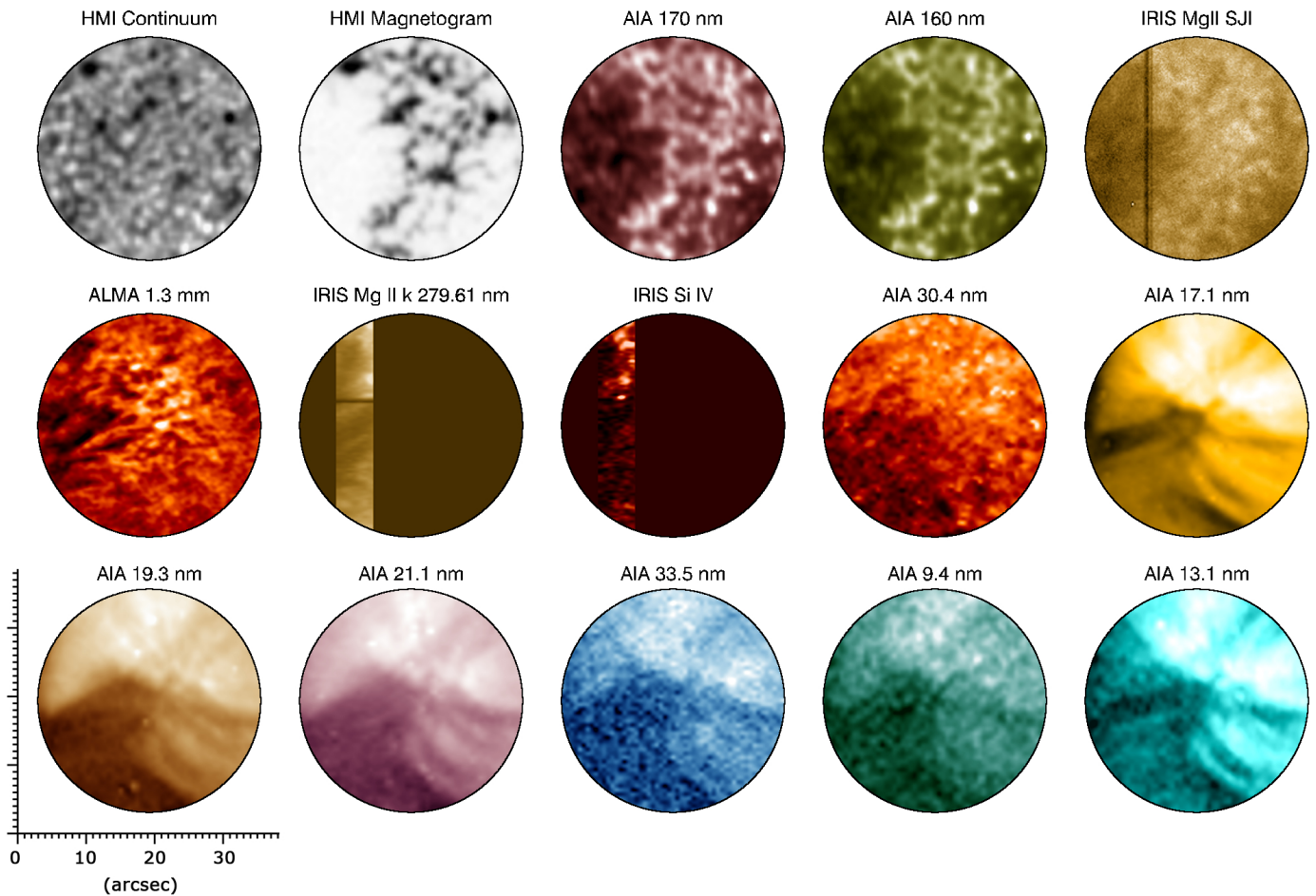[2] https://science.nrao.edu/facilities/vla/proposing/TBconv

**Fig. 4.** Same as Fig. 3, but for ALMA Band 6 taken on 2017 April 22 (project ID 2016.1.00050.S). In addition to the SDO channels, one slit-jaw image (SJI) and two raster images from IRIS are also displayed. Time series of images is available online as a movie.

For all sets except D01, self-calibration for phase (Cornwell & Fomalont 1999) was performed. For D01, the self-calibration method severely underperformed due to technical problems with pointing for those early observations. Spatial alignment (single shift value per frame, i.e. rigid) was performed for all sets except the limb set to effectively correct any residual jitter and wobbling of the time series. This follows a heavily adapted version of CRISPRED's polish tseries core routines (de la Cruz Rodríguez et al. 2015). Visually, the alignment procedure is generally successful in keeping features aligned and thus maximises science potential for time evolution studies.

The combining of total power and interferometric data was performed in different ways as the pipeline development progressed. The primary goal of this step is to obtain absolute brightness temperatures since the interferometer only provides differences (as the zero frequency of the Fourier space would require a zero distance between two antennas, which cannot be obtained). For D01 and D08, this combination follows a process known as 'feathering', as described in Stanimirovic (2002). This procedure consisted of rescaling a matching TP map to the interferometric pixel scale and adding those values pixel-wise (spatially matched) to the entire cube. This technique allows for compensation of the incomplete uv Fourier space sampling by the interferometer by adding the low-frequency spatial variation at the same time as the absolute temperature. This technique was also favoured in Chintzoglou et al. (2021b) as it is desirable to recover the low-frequency spatial scales. However, the interfer-

ometric maps are available at a cadence of 1–2 s, while only one or a few TP maps with many minutes in-between are usually available. Consequently, the lower spatial frequency scales, set by the TP, will be steady, while the high spatial frequency features as set by the interferometer evolve. This would impact the mapping of features evolving on the affected scales, with the effect becoming more severe for larger differences between the time at which the interferometric data was taken and the time at which the employed TP data were recorded. For this reason, save the few exceptions highlighted both here and in the metadata (see Sect. 4.1) of the data files, the combining was done by computing an average over $3 \times 3$ TP pixels at the location of the interferometric observations and merely adding it to the interferometric data. This simpler technique avoids the introduction of false low-spatial-frequency structures, but it reduces the low-spatial-frequency information. Depending on the science case, this is either an advantage or a disadvantage, and a user of interferometric data, including the one put forward in this database, should be aware of the different choices made for each set. Aside from this paper, the information on this step, can be found in extension 'PRPARA' (extension 2) of each FITS data file. For the few data sets for which no TP single-dish observations were available, the offsets were set to the default (quiet-Sun) value, also listed in the headers, of either 7300 K for Band 3 or 5900 K for Band 6 as suggested by White et al. (2017). The same was done for the limb set (D11) because the TP offset setting close to the limb is highly uncertain. The latter is due to an overshooting

pattern present when scanning the disc with a single dish and to small pointing differences leading to large changes in absolute observed temperature. Thus, the present limb set and any future releases of limb sets should only be used to study variations in temperature until the issue has been fixed. Each TP, as available in ASA, is itself calibrated by assuming that the average brightness temperature in a region around disc centre has a value of 7300 K for Band 3 or 5900 K for Band 6, again following White et al. (2017). We note that this is not the same as setting the total power of an interferometric time series calibrated with that map to this same value. The TP signal is impacted by any bright or dark features in the region targeted by the interferometric array and also beyond corresponding to the beam pattern. Even if there is a significant time difference between the TP scan and the interferometric observations, the activity levels and heliocentric angle alone will result in the offset extracted from the TP being different than the quiet-Sun disc-centre value. Significant limb brightening (10% for Band 3 and 15% for Band 6) was found at these wavelengths and specific bandpasses (Alissandrakis et al. 2017; Sudar et al. 2019) and is thus a contributing factor, captured via TP calibration, to the final observed brightness temperature of the released sets.

Multiple scans, that is, continuous observing periods, were combined whenever possible provided the target is the same and the time difference between scans is small. Because small time gaps are present between scans, the user should use the time stamps per frame when doing any time-dependent analysis to avoid any such gaps or otherwise missing frames (e.g. filtered-out bad frames) within the series.

A final step to further reduce high frequency noise consisted of smoothing in time. The smoothing function and size are listed in the FITS metadata. For this release, most sets received a final smoothing with a boxcar of five frames (so 5-to-10-s smoothing depending on the set cadence). This smoothing was found to be important to be able to release all time series at the highest cadence possible, but ongoing refinements may make such filtering obsolete for most sets added or revised in the future.

Coordinates of the observations are computed using the RA and DEC listed in each measurement set released by the ASA and the 'reference time', which is usually the time of the first solar pointing (first same-named source for the first science scan in the case of multiple solar targets). These measurement set coordinates are converted to helioprojective Cartesian (X,Y) coordinates in arcseconds by using the solar disc centre RA and DEC at the reference time. SoAP includes a routine for such conversions, but, for some data sets in this first release, the web interface of the ALMA Solar Ephemeris Generator (Skokić & Brajša 2019)[3] was used. The helioprojective coordinates, the reference time, and other useful coordinate information such as the 'P' angle (i.e. position angle of the solar north pole) are listed in the headers of each data file under the World Coordinate System A (see Appendix A). Due to pointing issues in the early cycles, a target-dependent error of up to 20 arcsec is expected to be present (private communication). The pointing accuracy was improved for sets where co-simultaneous observations (e.g. with SDO) allowed for a refinement of the actually observed coordinates. The listed coordinates are the corrected values whenever possible, but in principle, they should be taken with caution due to the possibility of persisting multi-arcsec offsets from actual coordinates.

## 4. Data products

SALSA is hosted[4] by the Science Data Centre at the University of Oslo, which also, among other services, provides Hinode data. In this section, we describe the general format and content of the data products and the selection of data sets provided in the first release of SALSA.

### 4.1. Data format and header standard

The ALMA data on SALSA is provided as flexible image transport system (FITS) files containing the brightness temperatures as five-dimensional data arrays (in units of Kelvin) and two extensions. The first two array dimensions are the usual spatial dimensions, the third is wavelength, the fourth is Stokes, and the fifth is time. This format was chosen in preparation for future data sets that will make use of all five dimensions, even though the data sets in this first release consist of continuum time series only (one wavelength, one Stokes component). The extension 'TIMEVAR' contains a binary table with time-variable information. The table is self-described in the headers of the extension and will be extended in future releases. At the time of this release, it consists of the beam properties and time tags for each frame present in the cube. The first element of the table is the major axis of ellipse used to describe the beam, the second the minor axis, the third is the beam position angle, and the fourth the time tag. Following Rots et al. (2015), the time tags are presented in seconds counting from DATEREF (not to be confused with REF_TIME), here set to the midnight at the start of the date of the observations (i.e. 00:00:00.000). These beam properties can be used to compute a proxy for angular resolution by taking the mean of the minor and major axes, and such information is provided in the headers under the ALMA keyword SPATRES. For this database, SPATRES varies from 0.77 arcsec to 4.11 arcsec. The time-dependent beam properties from the extension TIMEVAR should be considered for wave studies where very small scales are analysed.

The second extension, PRPARA, contains an ASCII table with parameter names, values, and descriptions for different processing steps. The processing steps are named in the header of the extension and also in the primary header of the file using SOLARNET's 'detailed description of all processing steps' formalism (Sect. 8.2 thereof) which can be identified by the PRXXXn keywords. These include information on the used versions of CASA, SoAP, and other relevant details concerning data processing. Together with the public release of SoAP, which is planned for the near future, this allows advanced users to not only reproduce the data but also potentially optimise the data reduction towards wanted properties; for example, prioritising brightness temperature over accurate reproduction of spatial structure. Further details on the headers and extensions is provided in the Appendices A and B. The files are compliant with the Flexible Image Transport System NASA standard version 3.0, 4.0, with the evolving ALMA header format standard (Felix Stoehr, priv. comm.), and the SOLARNET Metadata Recommendations document version 1.4 (Haugan & Fredvik 2020).

### 4.2. Data sets in the first SALSA release

All data sets that are included in the first release of SALSA are listed in Table 1. They all contain time series of continuum brightness temperature maps. Please note that data sets

---

for (quasi-static) mosaics can be retrieved directly from the ASA. For the data sets on SALSA, fundamental information such as date, band, helioprojective coordinates at the start of the time series, and identified co-observations are listed. In the first release, mostly co-observations with IRIS are considered as it is a highly complementary observatory, providing sampling of the transition region and chromosphere in high spectral resolution. Attempts by multiple observatories to coordinate with ALMA were made but not necessarily guaranteed or successful due to the common challenges of observations such as accurate pointing and timing. This was also the case for a few observations coordinated with IRIS that we found to not have overlapping target regions on the Sun. For example, for D22 the disc centre was observed by ALMA, which was not the coordinated target observed by IRIS. For D11, D16, D18, and D19, the correct targets were observed by IRIS but not at the same time as ALMA. A direct link to the specific IRIS observations page is provided on SALSA's web interface, which typically includes information on further observatories, including SDO and Hinode. The SALSA web-interface also provides the corresponding full-disc TP map of the Sun on which the location of the interferometrically observed region is marked. These are the TP maps used for calibration (multiple TP observations may exist per set). Such TPs are available from ASA, but are reproduced in SALSA for convenience and record completeness. As an exception, being an early set, D01's TP is only available in raw format at ASA but was processed in the same way as the remaining TPs for the production of D01 (described in Sect. 3). It is available as a final product at SALSA.

Some sets from SALSA have been reduced by other researchers independently of this database and were used in diverse publications. The reductions are not always comparable. A main point of difference is that we only release sets at high cadence, and other publications might consider averaged properties. The last column of Table 1 identifies all publications known to have used the same raw data (but with different processing) and publications for which sets from this database were used. The latter are marked in bold.

## 5. Obtaining and using SALSA data

### 5.1. SALSA

The data files in FITS format can be downloaded from SALSA[5] by accessing the webpage[6] and clicking 'download' in the appropriate column for each of the desired sets. Sets can be selected using their listed properties, either manually or by using the search bar on the top right of the table, by the quality and visible structures upon examination of the playable embedded movie (press 'movie' button), or by the location on the solar disc and respective context, as identifiable by the square marker overlaid on the image of the TP single-dish scan shown in the last column. The latter corresponds to the TP map used for total power calibration, as described in Sect. 3. The data arrays are ready to use in a form analogous to any other solar data, and they follow the format described in Sect. 4. The headers and extensions provide additional advanced information following the standard described in Appendices A and B.

### 5.2. SALAT

The Solar ALMA Library of Auxiliary Tools (SALAT[5]) enables easy loading and initial visualisation and exploration of SALSA data products in both Interactive Data Language (IDL) and Python. For a complete description of SALAT, installation guide and examples, please visit the corresponding webpage[7]. SALAT includes routines (IDL) and functions (Python) for reading the FITS files and extracting useful information such as arrays with the observing times or the synthesised beam shape for each ALMA image frame. It can be used to compute basic statistics for the time-series or individual frames, as well as for the corresponding ALMA synthesised beam, which are all important for advanced analysis. Functions to plot ALMA data, including the beam shape, and the possibility of saving the images are included. SALAT can also be used for identifying the best frames in an observation or to obtain a general idea of the timeline during the observation period, including any time gaps due to filtered-out frames or concatenated scan periods. Useful for the production of synthetic observables and comparison with co-observations, SALAT allows the usage of the ALMA beam of a particular observation to convolve it with other types of data, such as complementary data sets and simulations. Finally, SALAT can be used to create a new FITS file with the appropriate format (e.g. reduced dimensions), which can be inspected with other external viewing or analysis tools such as SAOImageDS9 (Joye & Mandel 2003), CARTA (Comrie et al. 2021), CRISPEX (Vissers 2012; Löfdahl et al. 2021), and so on.

## 6. Summary and outlook

We present the first release of SALSA – a database of 26 science-ready data sets for ALMA observations of the Sun. We also present the first release of SALAT, an IDL and Python package for loading and initial visualisation and exploration of SALSA data products. We plan to extend SALSA with additional data sets in the future. Depending on the further development of solar observing modes with ALMA, new data sets for new capabilities will be added. That includes, for instance, data measured in other receiver bands (e.g. Band 5 or 7), different frequency setup (e.g. sub-band sampling), mosaics, other antenna array configurations, but also different image reconstruction techniques.

---

# References

Alissandrakis, C. E., Patsourakos, S., Nindos, A., & Bastian, T. S. 2017, A&A, 605, A78

Alissandrakis, C. E., Nindos, A., Bastian, T. S., & Patsourakos, S. 2020, A&A, 640, A57

Bastian, T. S. 2002, Astron. Nachr., 323, 271

Bastian, T. S., Chintzoglou, G., De Pontieu, B., et al. 2017, ApJ, 845, L19

Bastian, T. S., Bárta, M., Brajša, R., et al. 2018, The Messenger, 171, 25

Brajša, R., Sudar, D., Benz, A. O., et al. 2018, A&A, 613, A17

Brajša, R., Skokić, I., Sudar, D., et al. 2021, A&A, 651, A6

Chintzoglou, G., De Pontieu, B., Martínez-Sykora, J., et al. 2021a, ApJ, 906, 82

Chintzoglou, G., De Pontieu, B., Martínez-Sykora, J., et al. 2021b, ApJ, 906, 83

Comrie, A., Wang, K. S., Hsu, S. C., et al. 2021, CARTA: The Cube Analysis and Rendering Tool for Astronomy

Cornwell, T., & Fomalont, E. B. 1999, in Synthesis Imaging in Radio Astronomy II, eds. G. B. Taylor, C. L. Carilli, & R. A. Perley, ASP Conf. Ser., 180, 187

da Silva Santos, J. M., de la Cruz Rodríguez, J., White, S. M., et al. 2020a, A&A, 643, A41

da Silva Santos, J. M., de la Cruz Rodríguez, J., Leenaarts, J., et al. 2020b, A&A, 634, A56

de la Cruz Rodríguez, J., Löfdahl, M. G., Sütterlin, P., & Hillberg, T. 2015, & Rouppe van der Voort. L., A&A, 573, A40

De Pontieu, B., Title, A. M., Lemen, J. R., et al. 2014, Sol. Phys., 289, 2733

Dulk, G. A. 1985, ARA&A, 23, 169

Eklund, H., Wedemeyer, S., Szydlarski, M., Jafarzadeh, S., & Guevara Gómez, J. C. 2020, A&A, 644, A152

Eklund, H., Wedemeyer, S., Szydlarski, M., & Jafarzadeh, S. 2021, A&A, 656, A68

Greisen, E. W., & Calabretta, M. R. 2002, A&A, 395, 1061

Guevara Gómez, J. C., Jafarzadeh, S., Wedemeyer, S., et al. 2021, Phil. Trans. R. Soc. London Ser. A, 379, 20200184

Haugan, S. V. H., & Fredvik, T. 2020, https://doi.org/10.5281/zenodo.5719255

Högbom, J. A. 1974, A&AS, 15, 417

Jafarzadeh, S., Wedemeyer, S., Szydlarski, M., et al. 2019, A&A, 622, A150

Jafarzadeh, S., Wedemeyer, S., Fleck, B., et al. 2021. Phil.Trans. R. Soc. London Ser. A, 379, 20200174

Joye, W. A., & Mandel, E. 2003, in Astronomical Data Analysis Software and Systems XII, eds. H. E. Payne, R. I. Jedrzejewski, & R. N. Hook, ASP Conf. Ser., 295, 489

Karlický, M., Bárta, M., Dąbrowski, B. P., & Heinzel, P. 2011, Sol. Phys., 268, 165

Lemen, J. R., Title, A. M., Akin, D. J., et al. 2012, Sol. Phys., 275, 17

Löfdahl, M. G., Hillberg, T., de la Cruz Rodríguez, J., et al. 2021, A&A, 653, A68

Loukitcheva, M. A., Solanki, S. K., & White, S. 2008, Ap&SS, 313, 197

Loukitcheva, M. A., White, S. M., & Solanki, S. K. 2019, ApJ, 877, L26

Martínez-Sykora, J., De Pontieu, B., de la Cruz Rodriguez, J., & Chintzoglou, G. 2020, ApJ, 891, L8

McMullin, J. P., Waters, B., Schiebel, D., Young, W., & Golap, K. 2007, in Astronomical Data Analysis Software and Systems XVI, eds. R. A. Shaw, F. Hill, & D. J. Bell, ASP Conf. Ser., 376, 127

Menezes, F., Selhorst, C. L., Giménez de Castro, C. G., & Valio, A. 2021, ApJ, 910, 77

Molnar, M. E., Reardon, K. P., Chai, Y., et al. 2019, ApJ, 881, 99

Nindos, A., Alissandrakis, C. E., Bastian, T. S., et al. 2018, A&A, 619, L6

Nindos, A., Alissandrakis, C. E., Patsourakos, S., & Bastian, T. S. 2020, A&A, 638, A62

Nindos, A., Patsourakos, S., Alissandrakis, C. E., & Bastian, T. S. 2021, A&A, 652, A92

Patsourakos, S., Alissandrakis, C. E., Nindos, A., & Bastian, T. S. 2020, A&A, 634, A86

Pesnell, W. D., Thompson, B. J., & Chamberlin, P. C. 2012, Sol. Phys., 275, 3

Rau, U., & Cornwell, T. J. 2011, A&A, 532, A71

Rodger, A. S., Labrosse, N., Wedemeyer, S., et al. 2019, ApJ, 875, 163

Rots, A. H., Bunclark, P. S., Calabretta, M. R., et al. 2015, A&A, 574, A36

Schou, J., Scherrer, P. H., Bush, R. I., et al. 2012, Sol. Phys., 275, 229

Selhorst, C. L., Simões, P. J. A., Brajša, R., et al. 2019, ApJ, 871, 45

Shimojo, M., Bastian, T. S., Hales, A. S., et al. 2017a, Sol. Phys., 292, 87

Shimojo, M., Hudson, H. S., White, S. M., Bastian, T. S., & Iwai, K. 2017b, ApJ, 841, L5

Skokić, I., & Brajša, R. 2019, Rudarsko-geološko-naftni zbornik, 34, 59

Stanimirovic, S. 2002, in Single-Dish Radio Astronomy: Techniques and Applications, eds. S. Stanimirovic, D. Altschuler, P. Goldsmith, & C. Salter, ASP Conf. Ser., 278, 375

Stoehr, F., Manning, A., Moins, C., et al. 2017, The Messenger, 167, 2

Sudar, D., Brajša, R., Skokić, I., & Benz, A. O. 2019, Sol. Phys., 294, 163

Thompson, W. T. 2006, A&A, 449, 791

Valle Silva, J. F., Giménez de Castro, C. G., Selhorst, C. L., Raulin, J. P., & Valio, A. 2021, MNRAS, 500, 1964

Vissers, G., & Rouppe van der Voort, L. 2012, ApJ, 750, 22

Wedemeyer, S., Bastian, T., Brajša, R., et al. 2016, Space Sci. Rev., 200, 1

Wedemeyer, S., Szydlarski, M., Jafarzadeh, S., et al. 2020, A&A, 635, A71

White, S. M., Loukitcheva, M., & Solanki, S. K. 2006, A&A, 456, 697

White, S. M., Iwai, K., Phillips, N. M., et al. 2017, Sol. Phys., 292, 88

Wootten, A., & Thompson, A. R. 2009, IEEE Proc., 97, 1463

Yokoyama, T., Shimojo, M., Okamoto, T. J., & Iijima, H. 2018, ApJ, 863, 96

## Appendix A: Data file headers

The header keywords in the SALSA FITS files seek to ensure reproducibility of the data, facilitate easy search across the archive for data fulfilling specific criteria, and ensure the availability of critical metadata information in a standardised fashion that respects all the previous conventions. We specifically guarantee that the SALSA data format conforms to the FITS standard 3.0 and 4.0, the SOLARNET recommendations (under revision: Haugan & Fredvik 2020), representation of World Coordinates in FITS (Greisen & Calabretta 2002), World Coordinate System for Solar Observations (following Thompson 2006), and Rots et al. (2015) for time-coordinate representation in FITS files. The most recent evolving ALMA FITS data-product standard (Felix Stoehr, private communication) and ALMA memo 611 were also followed with slight departures from the memo where a collision was present. ALMA memo 613 was also used to inform decisions where two options were possible. Adaptation of existing keywords was necessary but kept to a minimum and never went against any standards. Three headers exist, one per HDU, with relevant keywords per extension.

The keywords are listed, per extension, in Tables A.1 and B.1, with an example and a short description. The helioprojective coordinates keywords are summarised in Table A.2. In the description of each keyword, we include the list of standards that constrain or originated its usage. These are abbreviated in the following way: F3.0 for NASA FITS Standard 3.0 (sometimes preferred in CASA documentation), F4.0 for NASA FITS Standard 4.0, T2006 for Thompson (2006), SNET for the SOLARNET recommendations document, S1.9 for the ALMA FITS data-product standard version 1.9, and A611 or A613 for ALMA memos 611 and 613, respectively.

World Coordinate System keywords are used according to Greisen & Calabretta (2002) and Thompson (2006) to describe the data coordinates in two separate coordinate systems. The primary coordinate system specifies RA/DEC in a SIN projection, and thus CTYPE1='RA—SIN' and CTYPE2='DEC–SIN'. The secondary coordinate system specifies helioprojective longitude and latitude in a gnomonic projection, and thus CTYPE1A = 'HPLN-TAN' and CTYPE2A = 'HPLT-TAN' (note suffix A in keyword names for the secondary system).

The existing CASA keywords were passed through at this stage unless they were set to be changed as per the most recent information regarding the ALMA FITS data-product standard. An example of this is the keyword ORIGIN, set in most archival data to be the CASA version where it should instead display the originating institution (in agreement with FS3.0 and FS4.0). In such cases, the header in SALSA data files is corrected.

**Table A.1.** Keywords used in all SALSA data products and respective description with examples.

| Keyword | Example Value | Description |
|---|---|---|
| | Generic FITS keywords common for all SALSA data products | |
| PROPCODE | '2018.1.01879.S' | Project code to which the data belongs. String. Set by S.19. |
| PROJECT | 'SolarALMA' | Project. String. Set by SNET. |
| INSTRUME | 'BAND3' | Band. String. Reserved by FS3.0. FS4.0. Set by S1.9. |
| FILENAME | 'solaralma.....image.fits' | Filename. String. Set by SNET. |
| DATAMIN | 5800 | Minimum value of the data. Float. Reserved and set by: F3.0, F4.0, SNET. |
| DATAMAX | 6100 | Maximum value of the data. Float. Reserved and set by: F3.0, F4.0, SNET. |
| CASAVER | 'CASA 3.4.0(release r19988)' | String. Set by S1.9 and A613. |
| ORIGIN | 'JAO-UIO' | UIO appended. String. Reserved by F3.0. F4.0. Set by S1.9. |
| SOLARNET | '0.5' | 0.5 or 1 for partially compliant or fully compliant. String. Set by SNET |
| PWV | 0.7 | Unit: mm. Average precipitable water vapour. Float. A quality metric. |
| SPATRES | 0.5 | Geometric average of the min and the max beam axes (a sort of "Spatial resolution"). Float. Arcsec. Set by A613 and S1.9. |
| BNDCTR | 2.315424966698E+11 | Center frequency of data in the FITS array. Hz. Set by S1.9 and SNET. |
| WAVEBAND | 'ALMA Band 3' | Human readable band description. SNET. |
| OBS_HDU | 1 | Contains Observational data. Integer. Set by SNET. |
| DATE-BEG | '2014-12-11T19:09:13' | Start of solar observations. String. Set by FS3.0 ,FS4.0, SNET. |
| DATATAG | 'This paper makes use of the following ALMA data: ADS/JAO.ALMA# [Project code]. ALMA is a partnership of ESO (representing its member states), NSF (USA) and NINS (Japan), together with NRC (Canada) and NSC and ASIAA (Taiwan), in cooperation with the Republic of Chile. The Joint ALMA Observatory is operated by ESO, AUI/NRAO and NAOJ. It also makes use of the Solar ALMA Science Archive developed at UiO and based on SoAP reduction. Please cite ...' | Set by S1.9. Implemented in SALSA as an OGIP 1.0 compliant LONGSTRN. |

**Table A.1.** continued.

| Keyword | Default Value | Description |
|---|---|---|
| | Primary HDU FITS keywords | |
| CREATOR | 'SoAP' | Name of the last software that created the data contents. String. Set by SNET. |
| VERS_SW | '0.12' | Version of the CREATOR software. String. Set by SNET. |
| HASH_SW | '424d417e04...' | Hash of CREATOR software (robust versioning). Can be GIT hub commit hash. Example is the hash for the latest version marked as v0.14. String. Making its way into SNET. |
| CO_OBS | 'IRIS 3640009423,SST,NST' | Comma separate list of telescopes with identified co-observations and strings of observation IDs if available. String. |
| CHNRMS | 0.324E-03 | Channel RMS. Kelvin. Float. Set by S1.9 and A613 (but not in Jy/beam). |
| FOV | 1.54 | Total area of the field of view of the image. Square degrees. Float. Set by S1.9. |
| EFFDIAM | 0.70 | Effective diameter of the field of view. Degrees. Float. Set by S1.9 |
| RES_MEAN | 0.1 | Mean of residuals after CLEAN. Float. Basic quality measure. |
| RES_STDV | 0.1 | Standard deviation of the residuals. Float. Basic quality measure. |
| VAR_KEYS | 'TIMEVAR; BMAJ, BMIN, BPA, TIME_TAG' | Reference to extension containing time-variable values. String. Set by SNET. |
| PRSTEP1 | 'CLEAN' | Processing steptype. Generic form is PRSTEPn where n stands for number of processing step. String. Set by SNET. |
| PRPROC1 | 'TCLEAN' | Name of procedure performing PRSTEP1. String. Set by SNET. |
| PRPVER1 | 0.8 | Version of procedure PRPROC1. String. Set by SNET. |
| PRREF1A | 'UIO-ALMA (solaralma@uio.no)' | Group doing manual adjustments. String. Set by SNET. |
| PRPARA1 | '[PRPARA]' | Name of extension containing list of parameters or options for PRPROC1. String. Set by SNET. |
| PRLIB1 | 'CASA ' | Software library containing TCLEAN. String. Set by SNET. |
| PRVER1 | 5.6 | Library version or Modified Julian Day (MJD) of last update. String. Set by SNET. |
| PRSTEP2 | 'TPCALIB' | PRocessing steptype. Generic form is PRSTEPn where n stands for number of processing step. Set by SNET. |
| PRPROC2 | 'SOAP_FEATHER' | Name of procedure performing PRSTEP1. String. Set by SNET. |
| PRPVER2 | 1.0 | Version of procedure PRPROC2. String. Set by SNET. |
| PRPARA2 | '[PRPARA]' | Name of extension containing list of parameters or options for PRPROC2. String. Set by SNET. |

**Table A.2.** World coordinate system keywords for solar imaging data used in SALSA. Generic keywords.

| Keyword | Default Value | Description |
|---|---|---|
| World Coordinate System - Helioprojective keywords |||
| WCSNAMEA | 'Helioprojective-cartesian' | Name of coordinate set. String. Set by T2006 and A611. |
| CTYPE1A | 'HPLN-TAN' | Axis labels. Set by T2006 and A611. |
| CTYPE2A | 'HPLT-TAN' | Axis labels. Set by T2006 and A611. |
| CRPIX1A | 180.5 | Reference pixel: center of image in pixels. Set by T2006 . |
| CRPIX2A | 180.5 | Reference pixel: center of image in pixels. Set by T2006. |
| CUNIT1A | 'arcsec' | Angles in arcsec. Set by T2006 and A611. Arcsec is allowed by WCS. |
| CUNIT2A | 'arcsec' | Angles in arcsec. Set by T2006 and A611. Arcsec is allowed by WCS. |
| CDELT1A | 0.55 | Plate scale (i.e. pixel size). Set by T2006. Here in arcsec as in A611. |
| CDELT2A | 0.55 | Plate scale (i.e. pizel size). Set by T2006. Here in arcsec as in A611. |
| CRVAL1A | 0.0 | Helioprojective x (solar x) coordinate of the reference pixel in arcsec. Set by T2006. Here in arcsec as in A611. |
| CRVAL2A | 0.0 | Helioprojective y (solar y) coordinate of the reference pixel in arcsec. Set by T2006. Here in arcsec as in A611. |
| CTYPE5 | 'TIME' | This is in relation to REF_TIME, per frame. Time found in TIME_TAG under extension TIMEVAR. |
| CUNIT5 | 's' | Unit for fifth axis. Seconds in relation to REF_TIME, per frame. Time found in TIME_TAG under extension TIMEVAR. Normally preceding midnight. |
| DSUN_OBS | 147296035413.001 | Distance between observer and Sun in meters. Set by T2006 and A611 with A611 precision. |
| RSUN_REF | 696000000.0 | Radius of the Sun in meters. Set by T2006 and A611 with A611 precision. |
| RSUN_OBS | 6.96e8 | Observed radius of the Sun in arcsec. Set by T2006 and A611 with tabled A611 precision. |
| HGLN_OBS | 0 | Heliographic longitude of the observer, in degrees. Set by T2006 and A611. |
| HGLT_OBS | −0.47 | Stonyhurst heliographic latitude of the observer, in degrees (in this coordinate set identical to the classical "$B_0$"). Set by T2006 and A611. |
| SOLAR_P | 11.6872 | Degrees. "rotate image by -solar P angle to get solar north up". Set by A611. |
| SOLAR_P0 | 11.6872 | Degrees. "rotate image by -solar P angle to get solar north up". Set by SNET. |
| REF_TIME | 2014-12-11T19:09:13 | Date and time. Time used for coordinate calculations. Set by A611. Note that, in the ASA scripts, this is typically "refTime", without the underscore. |

## Appendix B: Extension data

We used extensions for technical details regarding data reduction and time-varying information. The extension 'TIMEVAR' contains time-varying information stored in a standard binary table format. It follows the variable-keyword mechanism described in Appendix I-d of the SOLARNET recommendations. It can be selected programmatically by name (EXTNAME = 'TIMEVAR') and is referenced in the main header through the VAR_KEYS keyword. Its parameters are listed in Table B.1. These are the beam shape parameters BMAJ, BMIN, and BPA as functions of time and the time stamps (TIME_TAG) of each frame of the primary HDU. The TIME_TAG values are expressed in seconds from DATEREF following Rots et al. (2015).

The second extension, 'PRPARA', contains parameters that might change by data set for each processing step, stored as an ASCII table for readability. Code box B.3 presents a printout example of such an ASCII table from a specific file. The format is compatible with F3.0 and F4.0, and is included for the goal of reproducibility. The main header merely refers to that extension by its name in square brackets in the PRPARAnn keyword, as defined in the SOLARNET recommendations (described in Section 8.2 of the version currently under revision). The main header PRSTEPn keyword is used to specify the main methods used, for which the parameters in this ASCII table will be relevant. Table B.2 lists an example of a header of an extension containing such processing parameters. We note that these include a repetition of the PRxxxx keywords as also suggested by the SOLARNET recommendations. In the example printed out, the first 17 rows are spelled as in the CASA tclean routine call, as made by SoAP, and are recognisable in the general context of the CLEAN algorithm (the headers PRSTEP1). The remaining rows refer to other SoAP post-processing steps using native functions (the headers PRSTEP2).

**Table B.1.** Header of the extension with time-dependent variables, extension 'TIMEVAR', with example values. We note that the header keywords describe the variables in the binary table.

| Header of the extension containing time dependent variables. | | |
|---|---|---|
| Keyword | Default Value | Description |
| XTENSION | 'BINTABLE' | Type of extension. String. Set by F4.0. |
| TFIELDS | 4 | Total fields. Integer. Set by F4.0. |
| EXTNAME | 'TIMEVAR' | Name of the extension. String. Primary HDU refers to this name using VAR_KEYS |
| DATEREF | '2014-12-11T00:00:00' | Time in UTC. Reference time that sets the zero to all other UTC times such as the extension time stamps. String. Set by SNET and F4.0. |
| SOLARNET | 0.5 | SOLARNET compliance: 0.5 or 1 for partially compliant or fully compliant. Float. Set by SNET. |
| TTYPE1 | 'BMAJ' | First column. Beam shape major axis. Variable-keyword. String. Degrees. Set by F4.0. |
| TTYPE2 | 'BMIN' | Second column. Beam shape minor axis. Variable-keyword. String. Degrees. Set by F4.0. |
| TTYPE3 | 'BPA' | Third column. Beam average. Variable-keyword. String. Degrees. Set by F4.0. |
| TTYPE4 | 'TIME_TAG' | Fourth column. Tabulation of time. Variable-keyword. String. Set by F4.0. |
| TFORM1 | '1558E' | Real*4 (float). String. Set by F4.0 and SNET. |
| TFORM2 | '1558E' | Real*4 (float). String. Set by F4.0 and SNET. |
| TFORM3 | '1558E' | Real*4 (float). String. Set by F4.0 and SNET. |
| TFORM4 | '1558E' | Real*4 (float). String. Set by F4.0 and SNET. |
| TDIM1 | '(1,1,1,1,1558)' | Dimension of array. String. Set by F4.0 and SNET. |
| TDIM2 | '(1,1,1,1,1558)' | Dimension of array. String. Set by F4.0 and SNET. |
| TDIM3 | '(1,1,1,1,1558)' | Dimension of array. String. Set by F4.0 and SNET. |
| TDIM4 | '(1,1,1,1,1558)' | Dimension of array. String. Set by F4.0 and SNET. |
| TUNIT1 | 'arcsec' | Units for column 1. String. Set by F4.0 and SNET. |
| TUNIT2 | 'arcsec' | Units for column 2. String. Set by F4.0 and SNET. |
| TUNIT3 | 'arcsec' | Units for column 3. String. Set by F4.0 and SNET. |
| TUNIT4 | 's' | Units for column 4. String. Set by F4.0 and SNET. |

**Table B.2.** SALSA-specific header keywords for the extension containing processing parameters. Repetition from table 4.3 following direct recommendation from SOLARNET so that the main header does not need to be searched.

| Keyword | Default Value | Description |
|---|---|---|
| | | Extension data |
| EXTNAME | 'PRPARA' | Name of extension. This keyword is recognized by multiple libraries. String. Making its way to SNET. |
| PRSTEP1 | 'CLEAN' | Processing step type. Generic form is PRSTEPn where n stands for number of processing step. String. Set by SNET. |
| PRPROC1 | 'TCLEAN' | Name of procedure performing PRSTEP1. String. Set by SNET. |
| PRPVER1 | '0.8' | Version of procedure PRPROC1. String. Set by SNET. |
| PRREF1A | 'UIO-ALMA (solaralma@astro.uio.no)' | Group doing manual adjustments. String. Set by SNET. |
| PRPARA1 | '[PRPARA]' | Name of extension containing list of parameters or options for PRPROC1/PRPROC2. String. Set by SNET. |
| PRLIB1 | 'CASA ' | Software library containing TCLEAN. String. Set by SNET. |
| PRVER1 | '5.6' | Library version/MJD of last update. String. Set by SNET. |
| PRSTEP2 | 'TPCALIB' | Processing steptype. Generic form is PRSTEPn where n stands for number of processing step. String. Set by SNET. |
| PRPROC2 | 'SoAP+' | Name of procedure performing PRSTEP2. String. Set by SNET. |
| PRPVER2 | '1.0' | Version of procedure PRPROC2. String. Set by SNET. |
| PRREF2A | 'UIO-ALMA (solaralma@astro.uio.no)' | Group doing manual adjustments. String. Set by SNET. |
| PRLIB2 | 'SoAP' | Software library containing SALAT+. String. Set by SNET. |
| PRVER2 | '1.00' | Library version/MJD of last update. String. Set by SNET. |
| PRPARA2 | '[PRPARA]' | Name of extension containing list of parameters or options for PRPROC1 or PRPROC2. String. Set by SNET. |

```
      cellsize  [0.5 arcsec,0.5 arcsec]   Cellsize.String array input with units.
         Niter                   200000                     Number of iterations.
        robust                      0.5                            ROBUST. Float.
     cycleniter                     1000                      Cycleniter. Integer.
        pbmask                      0.3                            PBMASK. Float.
       pblimit                     True                       PBLIMIT. Always true.
       usemask                       pb               String. Usually set to "pb".
          gain                    0.025                              Gain. Float.
    deconvolver               multiscale                       DECONVOLVER. String.
    phasecenter                        0                 Always zero unless mosaic.
        scales                 [0,6,18]                    Scales. Integer array.
     weighting                    briggs                        Weighting. String.
        uvtaper          [0.0,0.2,0.3]        Float array. Smoothing parameters.
 smallscalebias                       ''       Smallscale bias. String, usually blank.
      normtype                flatnoise    Normalization type for residuals. String.
     threshold                     1 Jy           Stop threshold. String with units.
       gridder                 mosaicft         Mosaic as two arrays (12m 7m).
     mosweight                     True                        Bool. Always true.
   TPCalMethod        White et al. (2018)                   Calib method for TP.
    TPCalValue                     7300               Calib temperature for TP.
         REFTP       Xcc8b19_X4deb...manual   Identifier for calib TP. Abbreviated.
     CALIBTEMP                  7238.14         DC temperature level from TP.
     smoothfun                   BoxCar           PTseries smooth function.
    windowsize                 5 frames                  smooth w. size, frames.
    FiltMethods              RMS,Central           Methods for filtering frames.
         Nrefs                        4         Reference interval for alignment.
```

Code B.3:Example printout from extension PRPARA (extension 2), containing processing parameters for different steps. Referred to from the headers.